Mon. Not. R. Astron. Soc. **000**, 000–000 (1996)   Printed 4 October 1996

Accretion during binary star formation I. Ballistic accretion

Matthew R. Bate⋆

Institute of Astronomy, Madingley Road, Cambridge CB3 0HA

Accepted 1996 September 11. Received 1996 July 19, in original form 1996 February 21

ABSTRACT

We consider the effects of accretion, during binary star formation, on the mass ratio and separation of a 'seed' binary system. Numerical fragmentation calculations show that 'seed' binary systems may be formed during the gravitational collapse of molecular cloud cores. When initially formed, however, these protobinaries typically contain only a small fraction of the total mass of the cloud core. For the star formation process to reach completion, a protobinary system must grow in mass via accretion from the remainder of the infalling cloud. The accretion of, and interaction with, this matter affects the mass ratio, separation and eccentricity of the protobinary, and thus the final state of the system cannot be determined unless the effects of the accretion are known.

In this paper, the effects of accretion on the mass ratio and separation of an initially-circular protobinary system are determined as functions of the initial mass ratio of the protobinary and the specific angular momentum of the infalling cloud material. The effects are studied by modelling the cloud ballistically, with non-interacting particles which are accreted by the protostars. Qualitatively, it is found that the mass ratio and separation decrease for the accretion of low-specific-angular-momentum matter, and increase for the accretion of high-specific-angular-momentum material. The quantitative results, however, are found to depend critically on the assumed sizes of the protostars. As well as the effects on mass ratio and separation, the spin angular momentum of the accreted material is examined, and evidence is found that the circumstellar discs formed in a binary system may differ considerably between the two components. The implications for the formation of binary stellar systems are discussed.

Key words: accretion, accretion discs – binaries: general – circumstellar matter – methods: numerical – stars: formation

1 INTRODUCTION

In recent years, our knowledge of the statistical properties of binary stellar systems has greatly improved. This allows us to begin making direct comparisons between the predictions of theoretical star formation mechanisms and the observed statistics. From the main-sequence surveys of Duquennoy & Mayor (1991), Mayor et al. (1992) and Fischer & Marcy (1992) we know that most stars are in binary or multiple systems. Pre-main-sequence stars also occur primarily in binary systems (Mathieu, Walter & Myers 1989; Simon et al. 1992; Ghez, Neugebauer & Matthews 1993; Leinert et al. 1993; Reipurth & Zinnecker 1993) and even show an excess of companions over the main-sequence in most of the separation ranges surveyed. Thus, star formation must predominately produce multiple systems.

The database of the statistical properties of binary and multiple systems is steadily growing. These statistics can be used to test models of binary star formation. The Duquennoy & Mayor (1991) survey found that binary stars have separations ranging from a few $R_\odot$ to 10^4 AU, with a unimodal distribution and a broad peak at ≈ 30 AU. Furthermore, a relationship exists between the orbital period and eccentricity of the systems. Close binaries have circular orbits due to tidal circularization, while the maximum eccentricity of intermediate and long-period binaries increases with period, and there is a lack of long-period systems with eccentricities of less than 0.15. Finally, Duquennoy & Mayor (1991) found that the mass ratio distribution increases towards smaller mass ratios. There is also weak evidence that the mass ratio distributions may differ between short and long-period systems, with the distribution for short-period systems consis-

⋆ Present address: Max-Planck-Institut für Astronomie, Königstuhl 17, D-69117 Heidelberg, Germany tent with a uniform distribution, or possibly rising towards mass ratios of unity (Mazeh et al. 1992). This result is yet to be confirmed.

Over the past two decades, much effort has been put into theoretical studies of the formation of binary stellar systems. One of the many outcomes of this work is that fragmentation is the favoured mechanism for the formation of most binary systems. Two general types of fragmentation have been studied - thermal fragmentation (e.g. Boss & Bodenheimer 1979; Boss 1986; Bonnell et al. 1991, 1992; Bonnell & Bastien 1992; Myhill & Boss 1993; Nelson & Papaloizou 1993) and disc fragmentation (Adams, Ruden & Shu 1989; Shu et al. 1990; Heemskerk, Papaloizou & Savonije 1992; Woodward, Tohline & Hachisu 1994; Bonnell 1994; Bonnell & Bate 1994a, 1994b). Thermal fragmentation forms protobinary systems with separations ranging from 10 to 10^4 AU, which typically have large eccentricities and a wide variety of mass ratios. The fragmentation of protostellar discs, on the other hand, can form binaries with separations of order the disc size of $\lesssim$100 AU. This includes the formation of close protobinary systems (Bonnell & Bate 1994b) with separations of order 10 $R_\odot$. A variation of disc fragmentation also allows the fragmentation of a massive circumbinary disc to produce a multiple system (Bonnell & Bate 1994a; Burkert & Bodenheimer 1996).

A problem with past fragmentation studies has been that the calculations must be stopped soon after the fragments are formed. This is due to the enormous density contrast that develops during the collapse. The time steps required to evolve the calculations further are determined by the dynamic time scale of the gas within the fragments, which is many orders of magnitude shorter than the dynamic time scale of the collapsing cloud, and the calculations effectively grind to a halt. At this stage, the protobinary systems contain only a fraction of the total mass of the cloud. The size of this fraction depends on the separation of the binary, with the closer systems containing the least initial mass (Boss 1986). For long-period systems, the fraction is typically from $10 - 50$ per cent (e.g. Myhill & Boss 1993), while for close protobinaries the fraction may be less than 1 per cent (e.g. Bonnell & Bate 1994b). Before the final state of the stellar system is attained, the initial protobinary will grow in mass, and its orbital parameters will change due to the accretion of, and interaction with, the remaining cloud material. This makes it impossible to compare the results of these fragmentation calculations with observational statistics on binary stars.

Artymowicz (1983) studied the effects of accretion on a protobinary system. A binary was embedded within a collapsing 'gas' cloud, modelled by ballistic particles, and the effects of the accretion of this material on the binary's mass ratio and separation were studied. It was found that the effects depended primarily on the initial mass ratio of the binary, and the specific angular momentum of the infalling material. For the accretion of low-angular-momentum material the mass ratio and separation were found to decrease, while for high-angular-momentum accretion they increased. However, several areas require further study. First, Artymowicz primarily studied the effects on high-mass-ratio binaries. The effects on low-mass-ratio binaries need to be determined. Second, the effects that changing the sizes of the protostars and the initial radial-infall velocity of the 'gas' particles have on the results has not been adequately explored. Finally, the spin angular momentum accreted by the protostars, and the effects of accretion on the eccentricity of a binary are essentially unknown.

In this paper, the effects of ballistic accretion on a protobinary are determined over a much larger parameter space than Artymowicz (1983) studied. For each initial mass ratio, the effects on the binary's masses and separation are studied as a function of the specific angular momentum of the cloud. In addition, special interest is taken in the effects of varying the sizes of the protostars and the radial-infall velocity that 'gas' particles have when they are injected into the cloud. Finally, the accreted angular momentum for each component of the binary is determined. This quantity is important for the formation of circumstellar discs in a protobinary system. Eccentric binaries are not studied. The calculations were performed ballistically, rather than with dissipation, for two reasons. First, ballistic calculations require far less computation time compared to gaseous calculations. Second, we would like to know how important dissipation is, and under what circumstances the ballistic approximation is a good one for studying the effects of accretion on a binary. This will be the subject of a later paper, where the effects of gaseous accretion will be compared to the results presented here.

The ballistic particle code is described in Section 2. Details of the numerical calculations are given in Section 3. Section 4 gives the effects of ballistic accretion on the mass ratio of the protobinary. The effect on the binary's separation is discussed in Section 5, and the spin angular momentum accreted by each component is considered in Section 6. Section 7 contains a discussion of how the results are expected to be altered when gaseous, rather than ballistic, accretion is considered. Finally, in Section 8 the conclusions and observational implications are given.

2 COMPUTATIONAL METHOD

The calculations presented here were performed using a ballistic particle code derived from a smoothed particle hydrodynamics code (Bate, Bonnell & Price 1995; Bate 1995). A binary system, consisting of two point masses, is surrounded by a cloud of particles from which the binary can accrete. The particles are acted upon by gravitational forces from the binary's components only, with the back reaction on the binary included. No interparticle forces, such as pressure, viscosity, or self-gravity, are present. The equations of motion are integrated using a second-order Runge-Kutta-Fehlberg integrator with individual particle time steps. Individual time steps are calculated for each particle, and these are then binned into time steps which differ by a multiple of two from the minimum time step allowed by the code. The time step for each particle is limited by the Runge-Kutta-Fehlberg integrator tolerance. The integrator tolerance limits the changes in a particle's velocity and acceleration, between two time steps, to be less than a given tolerance (Bate et al. 1995). The tolerance is set by ensuring that the errors obtained in integrating a binary's orbit in the absence of 'gas' particles are negligible in comparison to the effects of accretion on the binary over the same period of time.

The point masses, modelling the protostars, accrete any 'gas' particles that fall within a certain radius, the accretion radius $r_{\rm acc}$, of them. The results are, therefore, expected to depend on the accretion radii of the protostars. This dependence is investigated.

3 NUMERICAL CALCULATIONS

The binary protostellar system is modelled by point masses as described above. The masses of the primary and secondary are M_1 and M_2, respectively. The binary has mass ratio $q = M_2/M_1$, total mass $M_{\rm b}$, and separation a. Only binaries with initially circular orbits are considered. Natural units are used with the gravitational constant $G = 1$ and, initially, $M_{\rm b} = 1$ and $a = D = 1$. For this choice of units, a specific angular momentum of unity corresponds to the specific angular momentum j that a 'gas' particle requires to form a circular orbit (in the absence of gravitational torques from the binary) about the centre of mass of the initial binary at a radius equal to the separation (i.e. $j_{\rm circ} = \sqrt{GM_{\rm b}D} = 1$).

The protobinary is embedded in a cloud of particles which models the gas cloud that remains after the binary's formation. These particles fall on to the binary system and are accreted by, or otherwise interact with, the binary. To maintain the cloud during a simulation, particles are injected at the outer boundary of the simulation at a radius $r = R$ from the binary's centre of mass. In all cases, the axis of rotation of the cloud is assumed to be the same as the axis of rotation of the binary and the cloud is either stationary, or is rotating in the same sense as the binary. Accretion from retrograde clouds is not studied. These assumptions are justified as it is envisaged that the infalling gas is from the cloud that the protobinary formed out of.

Artymowicz (1983) found the effects of accretion on a given binary vary mainly with the specific angular momentum of the infalling cloud material. Therefore, we specify that, in a given simulation, each particle is injected with the same specific angular momentum $j_{\rm inf}$. Thus, a particle's initial tangential velocity around the centre of mass is $v_{\rm t} = j_{\rm inf}/r_{\rm xy}$, where $r_{\rm xy}$ is the cylindrical radius from the axis of rotation of the binary.

In addition to the tangential velocity, the radial-infall velocity of the particles at the outer boundary of the calculation can be varied. This is set as some fraction $v_{\rm rad}$, of the radial velocity a particle would have after a free-fall from infinity

$$v_{\rm r} = v_{\rm rad}\sqrt{\frac{2GM_{\rm b}}{r} - \frac{j_{\rm inf}^2}{r_{\rm xy}^2}}, \tag{1}$$

where it is assumed that, for $v_{\rm rad} = 1$, the kinetic energy of the particle is equal to the gravitational energy liberated during its fall. The effect of varying $v_{\rm rad}$ is studied by performing some simulations with both $v_{\rm rad} = 0$ and $v_{\rm rad} = 1$. Note that increasing the radius of the outer boundary R, while keeping $v_{\rm rad} = 0$, has the same effect as maintaining the same boundary radius and increasing $v_{\rm rad}$.

For each simulation, the effects of accretion on the masses and orbit of the binary are determined by linear regressions of the accretion rates, mass ratio, and separation as functions of time. The linear regressions are performed only over the period of the simulation where steady-state accretion is attained. This provides the accretion rates $\dot{M}_1$, and $\dot{M}_2$, and the rates of change of the mass ratio $\dot{q}$ and the semimajor axis $\dot{a}$. Error estimates for each of these are obtained from the linear regression. For the accretion rates, these errors are combined with $\sqrt{N}/N$ statistical errors, where N is the number of particles accreted over the time period of the regression. These errors provide a good estimate of the true errors in the quantities. A second calculation of the rate of change of the mass ratio can be found, with a better estimate of errors, from

$$\dot{q} = (\dot{M}_2 - q\,\dot{M}_1)\frac{(1+q)}{M_{\rm b}}. \tag{2}$$

Note that this means the mass ratio increases if

$$\frac{\dot{M}_2}{\dot{M}_1} > q, \tag{3}$$

and not simply when $\dot{M}_2 > \dot{M}_1$.

Due to the absence of dissipation in the ballistic calculations, many of the particles fall towards the binary and then are expelled again since they do not pass within a protostellar accretion radius. Thus, the results depend to some degree on the chosen size of the protostars. This dependence is investigated by performing calculations with point mass accretion radii of 1/20 of the initial binary separation, and with sizes equal to the mean-Roche-lobe sizes of the protostars. These two cases are extremes that the true protostellar sizes should lie between. For example, although for a binary with an intermediate or wide separation the physical sizes of the protostars may be very much less than their separation, the formation of circumstellar discs around the two components may increase their effective sizes to be similar to their mean-Roche-lobe sizes. The mean-Roche-lobe sizes of the protostars are taken to be (Frank, King & Raine 1985)

$$R_1/a = 0.38 - 0.20\,\log\,q, \qquad 0.05 < q \leq 1, \tag{4}$$

for the primary and

$$\begin{aligned} R_2/a &= 0.38 + 0.20\,\log\,q, &\quad 0.5 \leq q < 1, \\ R_2/a &= 0.462\,\left(q/(1+q)\right)^{1/3}, &\quad 0 < q < 0.5, \end{aligned} \tag{5}$$

for the secondary. They are fixed at their initial values throughout a calculation as the total mass of material falling on to the system is much less than the initial mass of the binary and, thus, the binary's mass ratio and separation change by only a few percent.

In each simulation, the gas cloud is modelled by 5000 particles each of which has a mass $m = 10^{-6}M_{\rm b}$. When a particle is accreted by one of the protostars, it is randomly assigned a new position at the outer boundary of the calculation and is given a new velocity. As the particles are ballistic, it is also possible that they are expelled via a three-body interaction with the binary. To maintain a cloud of 5000 particles, any particle that passes outside the outer boundary is removed and its position and velocity are reassigned as for an accreted particle. A calculation is evolved until all memory of the initial conditions is lost, and steady-state accretion on to both protostars is established. At this point, the accretion rates and effects on the binary's orbital parameters are calculated. In a typical calculation 1.5×10^4 particles are accreted by the protostars. The number of particles that fall on to the system but are expelled,

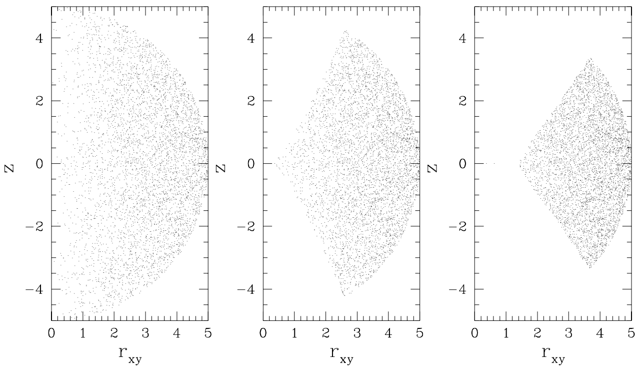

Figure 1. The initial particle distributions for calculations of ballistic accretion from clouds with specific angular momenta of $j_{\rm inf} = 0$ (left), $j_{\rm inf} = 0.6$ (centre), and $j_{\rm inf} = 1.2$ (right) on to a protobinary. For a stationary cloud the distribution is spherical. As the specific angular momentum is increased, particles are absent near the poles as the gravitational forces on them would be exceeded by centrifugal forces. Distance is expressed in units of the initial binary separation D.

rather than being accreted, depends primarily on the sizes of the accretion radii and the angular momentum of the infalling material and varies from 1/10 to 4 times the number of particles that are accreted by the protostars.

The initial particle distribution and reassignment of particles when they are accreted or removed is now discussed. Due to the rotation of the cloud, each particle has a centrifugal acceleration acting upon it. Clearly, any position in the cloud for which the centrifugal acceleration is not balanced or exceeded by the acceleration due to gravity of the binary should not initially be occupied by gas as it would not have been able to fall into this region from farther out in the cloud. Thus, we set the initial 'gas' particle positions to be randomly distributed within a sphere of radius R, such that

$$\frac{v_{\rm t}^2}{r_{\rm xy}} \leq \frac{GM_{\rm b}}{r^2}\frac{r_{\rm xy}}{r}, \qquad (6)$$

where r is the radius of a particle from the centre of mass of the binary. In the case of a stationary cloud, the whole sphere is filled. As the angular momentum of the cloud is increased, a cone-shaped hole in the particle distribution appears above and below the orbital plane of the binary. Several different particle distributions are shown in Fig. 1.

As particles are accreted by the binary, or expelled out to $r > R$, they are assigned new positions and velocities to maintain the cloud of infalling particles. We assign them new positions over the surface of the sphere of radius R, such that they have a uniform-density distribution modified by equation (6). Thus, for $j_{\rm inf} > 0$, the poles of the sphere receive no particles. Most calculations have the outer boundary of the calculation equal to five times the initial binary separation $R = 5D$.

Calculations were performed, varying the initial mass ratio of the binary, the cloud's angular momentum, the accretion radii of the point masses (protostars), and the radial-infall velocity at the outer boundary of the calculation. A few simulations were also performed to confirm that the results are scale-free under increase of the binary separation, increase of the total mass of the binary, and increase of the mass of the 'gas' particles (the gas cloud has a mass very much less than that of the binary). The accretion rates increase linearly with the total mass of the binary, and with the mass of the 'gas' particles, as expected. Also, the results for the relative accretion rate on to the binary components are the same, within statistical errors, for simulations where the separation of the binary is increased by a factor f, and the angular momentum of the cloud is increased in proportion to $\sqrt{f}$. In these cases, the accretion radii of the point masses is also increased by f.

The effects of accretion on orbital eccentricity are not studied, as the binaries are all in circular orbits initially. In all cases, however, a small eccentricity grows at the beginning of each simulation since eccentricity is always positive and, thus, any force on the binary produces a non-zero eccentricity. Hence, as soon as a particle is accreted, giving mass and momentum to the protostar, a non-zero eccentricity is produced. For all simulations, however, the eccentricity remains small ($e < 0.006$) throughout. The evolution of this eccentricity is for it to grow initially, and then to oscillate in a sinusoidal pattern with an approximately constant amplitude. The period of the oscillation is equal to the orbital period of the binary. The same behaviour was noted by Artymowicz (1983). Such periodic changes of orbital elements are known from analytic solutions of binary motion under a perturbing force (Kopal 1959). The oscillations of eccentricity display no noticeable dependence on the mass ratio of the binary, or the accretion radii of the components, but the amplitude decreases with increasing angular momentum of the cloud.

The effects of accretion on the binary are normalised by the total accretion rate on to the binary $\dot{M}_{\rm b} = \dot{M}_1 + \dot{M}_2$ and not the mass infall rate through the outer boundary $\dot{M}_{\rm inf}$, because different fractions of the injected particles are accreted or removed in each simulation. Furthermore, in reality, with gaseous accretion, some of the material may not be accreted by the protostars or their circumstellar discs, but instead may form a circumbinary disc and in this case $\dot{M}_{\rm b} < \dot{M}_{\rm inf}$. Hence, the quantities $\dot{q}/\dot{M}_{\rm b}$, $\dot{a}/\dot{M}_{\rm b}$ are used in the ballistic analysis. Note that since $a = 1$ and $M_{\rm b} = 1$ initially, then $\dot{M}_{\rm b}$ and $\dot{a}$ are also the fractional changes in $M_{\rm b}$ and a with time. Thus, $\dot{q}/\dot{M}_{\rm b} = \dot{q}/(\dot{M}_{\rm b}/M_{\rm b})$ and $\dot{a}/\dot{M}_{\rm b} = (\dot{a}/a)/(\dot{M}_{\rm b}/M_{\rm b})$.

4 EFFECTS OF ACCRETION ON THE BINARY MASSES

The effects of accretion on the masses of the binary's components are now considered. Calculations of accretion on to binary systems with mass ratios $0.1 \leq q \leq 1$ were performed, with the specific angular momenta of the clouds lying in the range $0 \leq j_{\rm inf} \leq 1.4$ for each mass ratio. In each case, two values of the accretion radii ($r_{\rm acc} = 0.05D$ and $r_{\rm acc}$ equal to the mean-Roche-lobe sizes) were used to test how the assumed accretion radius affects the results. Finally, for each case with $r_{\rm acc} = 0.05$, calculations were performed with both $v_{\rm rad} = 0$ and $v_{\rm rad} = 1$ to investigate the sensitivity of the results to the radial-infall velocity of the cloud material at the outer boundary of the calculations. With the mean-Roche-lobe-sized protostars, the calculations had $v_{\rm rad} = 1$.

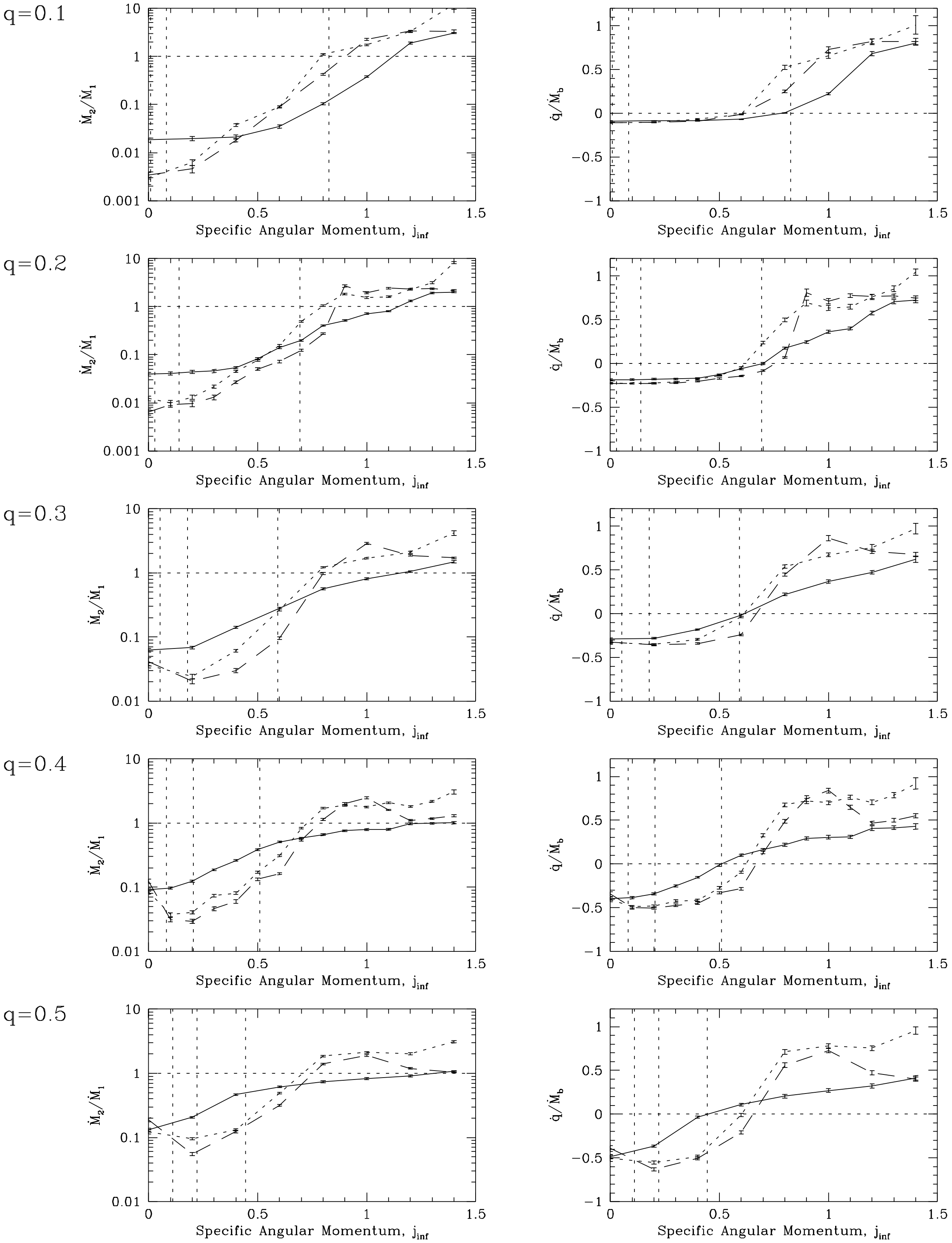

Figure 2. The a) relative accretion rates $\dot{M}_2/\dot{M}_1$ (left), and b) rates of change of mass ratio per unit fractional mass accreted $\dot{q}/\dot{M}_\mathrm{b}$ (right), for binaries with mass ratios $0.1 \leq q \leq 0.5$ accreting gas with specific angular momentum j_inf. The different curves are for calculations with mean-Roche-lobe-sized accretion radii r_acc and with radial-infall velocity $v_\mathrm{rad} = 1$ (solid), or $r_\mathrm{acc} = 0.05D$ with $v_\mathrm{rad} = 0$ (dotted) and $v_\mathrm{rad} = 1$ (dashed). The vertical lines give the specific angular momenta of the primary j_1 (left), binary j_b (centre), and secondary j_2 (right).

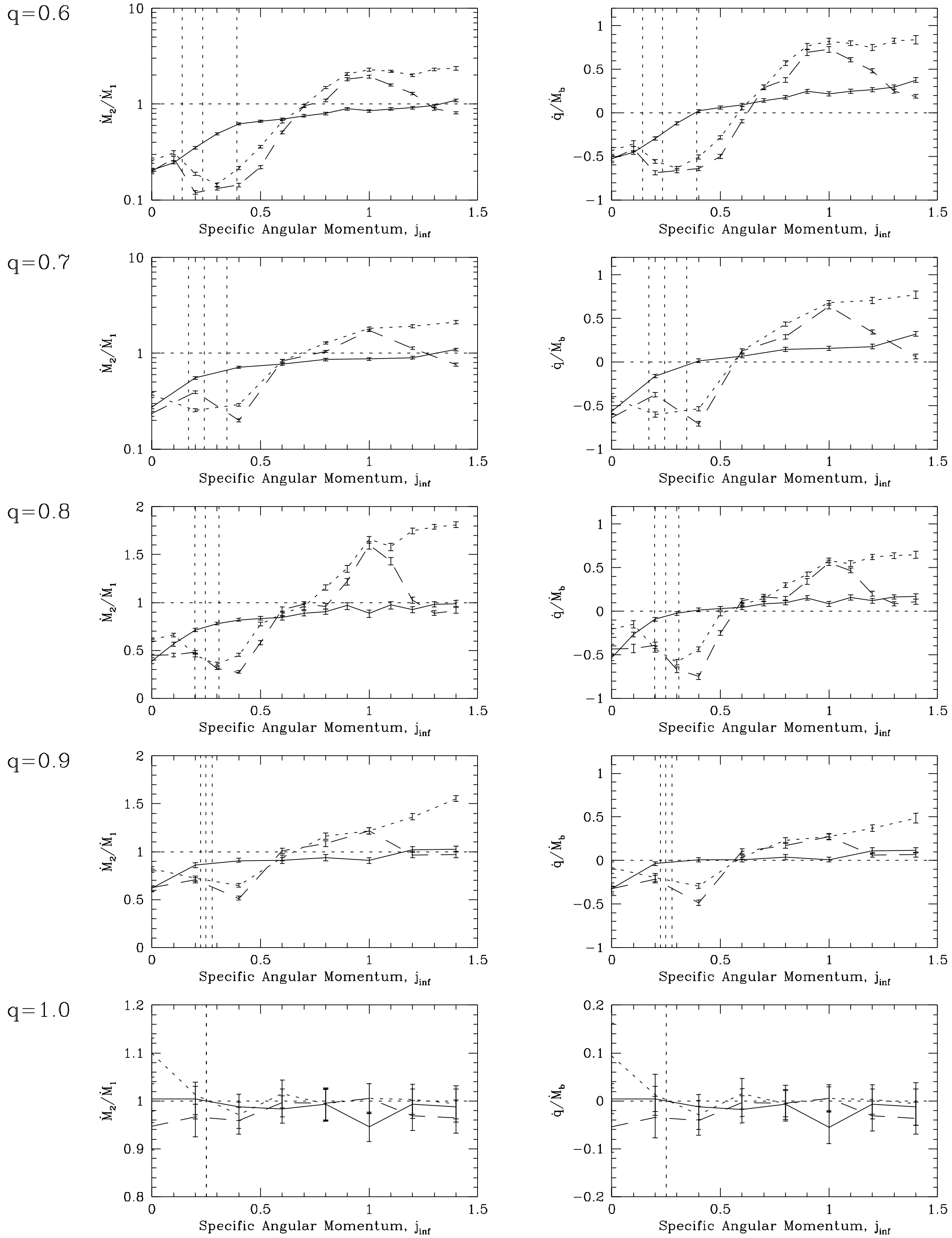

Figure 3. The a) relative accretion rates $\dot{M}_2/\dot{M}_1$ (left), and b) rates of change of mass ratio per unit fractional mass accreted $\dot{q}/\dot{M}_{\rm b}$ (right), for binaries with mass ratios $0.6 \leq q \leq 1.0$ accreting gas with specific angular momentum $j_{\rm inf}$. The different curves are for calculations with mean-Roche-lobe-sized accretion radii $r_{\rm acc}$ and with radial-infall velocity $v_{\rm rad} = 1$ (solid), or $r_{\rm acc} = 0.05D$ with $v_{\rm rad} = 0$ (dotted) and $v_{\rm rad} = 1$ (dashed). The vertical lines give the specific angular momenta of the primary j_1 (left), binary $j_{\rm b}$ (centre), and secondary j_2 (right).

4.1 Relative accretion rate and rate of change of mass ratio

The relative accretion rate $\dot{M}_2/\dot{M}_1$, and the rate of change of mass ratio per unit fractional mass accreted $\dot{q}/\dot{M}_{\rm b}$ are given for each mass ratio separately in Figs. 2 and 3.

In all cases, except for a mass ratio of unity, the trend determined by Artymowicz (1983) applies. For low-angular-momentum infall most material is accreted by the primary, while for high-angular-momentum infall the secondary accretes at least as much as the primary, and in many cases more. This can be understood by considering the trajectories of the infalling particles. For low-angular-momentum infall, most particles fall approximately radially towards the centre of mass of the binary. With a low-mass-ratio binary, these particles are mainly accreted by the primary, which is closest to the centre of mass of the system (e.g. $q = 0.1$ in Fig. 2). Few particles pass close to the secondary and are accreted by it, especially for small-accretion-radius calculations. With high-angular-momentum infall, however, the particles fall on elliptical orbits with their periastron distance dependent on their initial angular momentum and energy. They no longer fall into the centre of mass of the binary, occupied by the primary, but instead to some larger radius. Thus, less of the material is accreted by the primary, and more by the secondary. The primary can only accrete material that loses angular momentum and falls closer to it.

In all cases, the maximum accretion on to each component of the system occurs at a value of $j_{\rm inf}$ that increases with the distance of the component from the centre of mass of the binary. Thus, the maximum and minimum relative accretion rates are most extreme for low-mass-ratio binaries (e.g. $q = 0.1$, Fig. 2a). For accretion on to a low-mass-ratio binary, the relative accretion rate can vary between ≈ 0.003 and ≈ 10 depending on the angular momentum of the infalling material and the sizes of the protostars! As the mass ratio is increased, the relative accretion rates become less extreme (converging to unity for $q = 1$) since the primary and secondary become more equal, both in mass and in radius from the centre of mass. For the small-accretion-radii calculations, it is found that the value of the cloud's angular momentum for which the relative accretion rate is unity is only weakly dependent on the mass ratio. The relative accretion rate is unity when $j_{\rm inf} \approx 0.6 - 0.9$. For the mean-Roche-lobe-sized calculations, $j_{\rm inf} \gtrsim 1.1$ is required for a relative accretion rate greater than unity. Further discussion of this observation is contained in Section 4.2.

Note that in most calculations a significant fraction of the ballistic particles are not accreted either by the primary or secondary. This fraction increases both with increasing $j_{\rm inf}$, and also with decreasing $r_{\rm acc}$. Many particles fall in, interact with the binary, and then travel out and are removed at the outer boundary. This is an artifact of studying accretion ballistically. With gaseous accretion, all particles would dissipate their excess kinetic energy and be captured by the binary, either being accreted, or forming discs.

Of greatest significance to the evolution of the binary is the rate of change of mass ratio - specifically when $\dot{q}/\dot{M}_{\rm b}$ changes sign (Figs. 2b and 3b). Interestingly, for all mass ratios less than unity this seems to occur for approximately the same value of the cloud angular momentum of $j_{\rm inf} \approx 0.6 - 0.7$ with small-accretion-radii protostars. Below this value, the mass ratio decreases, above it increases. The rate of change of $\dot{q}/\dot{M}_{\rm b}$ is also most rapid when $\dot{q}/\dot{M}_{\rm b} \approx 0$. This implies that, under *constant*-specific-angular-momentum infall and if the separation of the binary remains unchanged, the binary is either driven to a very low mass ratio (for $j_{\rm inf} \lesssim 0.5$) or equal masses (for $j_{\rm inf} \gtrsim 0.6$). In reality, of course, the angular momentum of the cloud material is not expected to remain constant, and the binary's separation may evolve (see Section 5).

For protostars with mean-Roche-lobe sizes, the value of $j_{\rm inf}$ for which $\dot{q}/\dot{M}_{\rm b}$ changes sign does depend on the mass ratio - it occurs at lower $j_{\rm inf}$ when the mass ratio is increased. This again implies that, in the absence of changes in the binary's separation and the angular momentum of the cloud material, a binary whose mass ratio is decreasing continues to have it decrease, and a binary whose mass ratio is increasing continues to have it increase. The empirical relation that $\dot{q}/\dot{M}_{\rm b} = 0$ when $j_{\rm inf}$ is equal to the specific orbital angular momentum of the secondary j_2 (for $q < 1$) fits the mean-Roche-lobe ballistic accretion results very well. The specific orbital angular momenta of the primary and secondary are given by

$$j_1 = \sqrt{GM_{\rm b}a}\ \frac{q^2}{(1+q)^2} \tag{7}$$

and

$$j_2 = \sqrt{GM_{\rm b}a}\ \frac{1}{(1+q)^2} \tag{8}$$

respectively. For $j_{\rm inf} < j_2$, the mass ratio decreases, while for $j_{\rm inf} > j_2$ it increases.

Finally, as the mass ratio is decreased below $q = 0.4$, the magnitude of $\dot{q}/\dot{M}_{\rm b}$ decreases for low-angular-momentum infall. This reflects the fact that as the mass ratio decreases, the mass of the primary must be increased more and more for the mass ratio to decrease by the same amount. This is apparent if the limits of equation (2) are taken. If all the mass falls on to the primary (low $j_{\rm inf}$), then $\dot{q}/(\dot{M}_{\rm b}/M_{\rm b}) = -q(1+q)$, which tends to zero as $q \to 0$. If all the mass falls on to the secondary (high $j_{\rm inf}$), then $\dot{q}/(\dot{M}_{\rm b}/M_{\rm b}) = (1+q)$. Note that in practice this means that the maximum value of $\dot{q}/(\dot{M}_{\rm b}/M_{\rm b}) \approx 1$, since, as q increases, accretion on to the two components becomes more equal and ultimately the same for $q = 1$.

4.2 Dependence on accretion radii and the radial-infall velocity

The results presented in the previous section are from calculations performed with accretion radii of either 1/20 the initial separation D, or the mean-Roche-lobe sizes of the protostars. We now discuss the effects of varying the accretion radii $r_{\rm acc}$, and the radial-infall velocity $v_{\rm rad}$.

The protostellar radii used by Artymowicz (1983) were given by

$$R_{\rm i} = R_0 M_{\rm i}^n \tag{9}$$

where $M_{\rm i}$ are the masses of the stars, and n was varied between $-1/3 < n < 1/3$. Artymowicz found the results do not dependent significantly on the value of n. Unfortunately, it is not stated what R_0 was in terms of the binary separation,

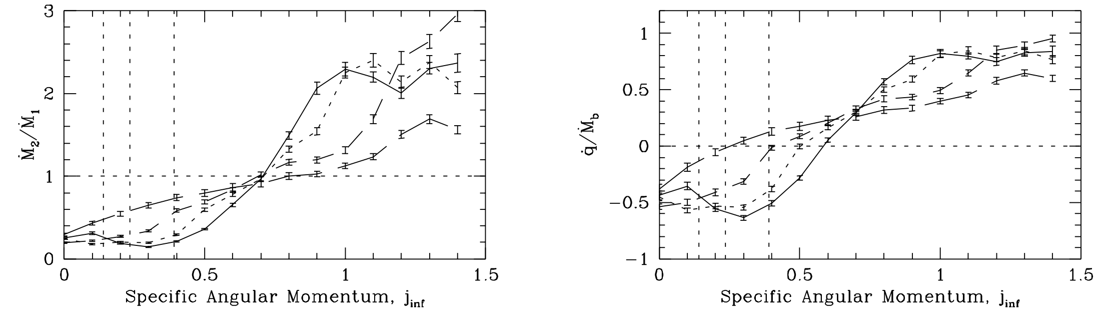

Figure 4. The a) relative accretion rates $\dot{M}_2/\dot{M}_1$ (left), and b) rates of change of mass ratio per unit fractional mass accreted $\dot{q}/\dot{M}_{\rm b}$ (right), for a $q = 0.6$ binary accreting 'gas' with specific angular momentum $j_{\rm inf}$. The calculations were performed with radial-infall velocity $v_{\rm rad} = 0$ and accretion radii of $r_{\rm acc} = 0.05D$ (solid), $r_{\rm acc} = 0.10D$ (dotted), $r_{\rm acc} = 0.20D$ (dashed), $r_{\rm acc} = 0.40D$ (long-dashed). The vertical lines give the specific orbital angular momenta of the primary j_1 (left), binary $j_{\rm b}$ (centre), and secondary j_2 (right).

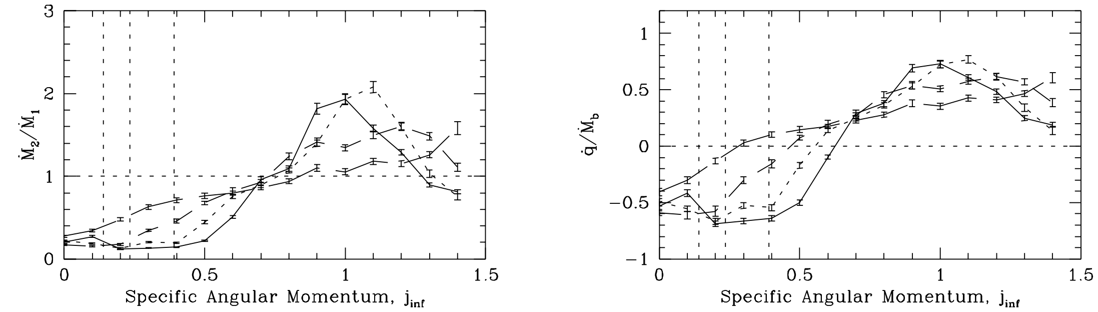

Figure 5. As in Fig. 4, except that the calculations were performed with a radial-infall velocity of $v_{\rm rad} = 1$.

or if this was changed. In the following analysis, we set $n = 0$ for all simulations, and only the value of $R_0 = r_{\rm acc}$ is varied.

To determine the dependence on protostellar accretion radius, an intermediate mass ratio of $q = 0.6$ is chosen which allows comparison to the results of Artymowicz (1983). Additional simulations were performed varying the cloud's angular momentum in the range $0 \leq j_{\rm inf} \leq 1.4$ as before, and, for each of these, varying the stellar accretion radius in multiples of two from $r_{\rm acc} = 0.05D$ to $r_{\rm acc} = 0.40D$. Calculations were also performed with $v_{\rm rad} = 0$ and $v_{\rm rad} = 1$ to examine the dependence on the radial-infall velocity. The results are presented in Figs. 4 and 5.

The relative accretion rates depend greatly on the accretion radius. Generally, the range of values decreases with increasing accretion radius with the relative accretion rate tending toward unity for very large accretion radii for all values of $j_{\rm inf}$. For $r_{\rm acc} = 0.40D$, the relative accretion rates are constrained to $0.3 \lesssim \dot{M}_2/\dot{M}_1 \lesssim 1.7$ for all values of $j_{\rm inf}$. Note that the value of $j_{\rm inf}$ for which the relative accretion rate is unity is *independent* of the accretion radius at $j_{\rm inf} \approx 0.7$. In the previous section it was also noted that, for $r_{\rm acc} = 0.05D$, the value of $j_{\rm inf}$ for which the relative accretion rate is unity depends only weakly on the mass ratio. However, these relations are true only if the two protostars have the same sizes; when the mean-Roche-lobe sizes are used, they disappear. For $q \gtrsim 0.4$ with mean-Roche-lobe sizes, the secondary appears never to accrete significantly more than the primary, even for angular momentum as high as $j_{\rm inf} = 1.4$ (Figs. 2a and 3a). This is because the secondary, being smaller in radius than the primary, accretes less. The specific angular momentum of the infalling material must be very large before the reduction in the secondary's size is compensated for and a relative accretion rate of unity is surpassed.

Comparing the results to those of Artymowicz (compare Figs. 4 and 5 to Fig. 4 of Artymowicz (1983)), a good match is only attained for a large value of $r_{\rm acc}$. For small $r_{\rm acc}$, the relative accretion rate changes rapidly for intermediate values of $j_{\rm inf}$. Artymowicz's results, however, give a 'plateau' at a relative accretion rate near unity for intermediate cloud angular momenta. This is only reproduced in Figs. 4a and 5a for $r_{\rm acc} \approx 0.40D$. Thus, Artymowicz must have used a large protostellar size in comparison with the binary separation. Since he was mainly considering accretion on to close binaries, this may not be a bad approximation, especially if during their formation the stars are surrounded by large discs. For wide binaries, however, the appropriate protostellar size is debatable. Gaseous accretion calculations are needed to resolve this issue.

For the rate of change of mass ratio (Figs. 4b and 5b), the effect of increasing the accretion radii is the same as that for the relative accretion rate - the range of $\dot{q}/\dot{M}_{\rm b}$ decreases. Also, the value of $j_{\rm inf}$ for which $\dot{q} = 0$ decreases with increasing $r_{\rm acc}$. This shifting toward lower $j_{\rm inf}$ should only be important for high mass ratios in reality, however, because for small mass ratios the secondary's size should be limited to its Roche-lobe size. This is apparent in Figs. 2b and 3b where, for the mean-Roche-lobe-sized calculations, only high mass ratios have $\dot{q} = 0$ at low $j_{\rm inf}$.

Therefore, the results given in the previous section should be viewed as giving the extremes of the relative accretion rate: if the appropriate sizes of the protostars are small, the ballistic results with $r_{\rm acc} = 0.05D$ will compare closest to the true behaviour of the system, while the behaviour with the largest possible sizes of the protostars and/or their circumstellar discs should be given by the mean-Roche-lobe-sized results. If the appropriate sizes are somewhere in between, the trends discussed above will give an idea of correct relative accretion rates.

Artymowicz (1983) also stated his results were independent of the radial-infall velocity. From the figures, changing the radial-infall velocity at the outer boundary has only a small effect for $j_{\rm inf} \lesssim 1$. For $j_{\rm inf} \gtrsim 1$, however, the relative accretion rate and $\dot{q}/\dot{M}_{\rm b}$ decrease as $v_{\rm rad}$ increases. This is easily understood by considering the trajectories of the 'gas' particles once again. With a higher $v_{\rm rad}$, the particles are on more elliptical trajectories, with smaller periastron distances, and thus are more easily accreted by the primary which is closer to the binary's centre of mass. Even for $j_{\rm inf} \lesssim 1$ this effect is visible in the small-accretion-radii calculations, with $\dot{M}_2/\dot{M}_1$ generally smaller for $v_{\rm rad} = 1$ than with $v_{\rm rad} = 0$ (Figs. 2 and 3). The effect is more important, however, for high $j_{\rm inf}$ where the difference in periastron distance determines whether or not the particles fall inside the secondary's orbit. Finally, the effect of the radial-infall velocity depends on the sizes of the protostars. For large protostars, $v_{\rm rad}$ has little effect on the results because the secondary intercepts much of the infalling material before it gets to the primary regardless. Thus, if the sizes of the protostars depend on their masses (e.g. their Roche-lobe sizes) the radial-infall velocity is expected to affect the results more for low mass ratios than high mass ratios since the secondary is smaller.

5 EFFECTS OF ACCRETION ON THE BINARY SEPARATION

Accretion on to a binary affects not only the masses, but also the orbital elements of the system. The effect on the separation of the binary is investigated using results from the same simulations as in Section 4.

5.1 Total effect of ballistic accretion

If the change in separation was due only to the accretion of particles by the binary, then $\dot{a}/\dot{M}_{\rm b}$ from the calculations would be sufficient to give $\dot{a}$ for a known accretion rate on to the binary. However, with ballistic accretion, not all of the injected particles are accreted. Many, as discussed previously, fall toward the binary, gain angular momentum and/or energy, and then are expelled from the system. When such a particle is removed, there is a loss of angular momentum from the system, and the binary loses whatever angular momentum the particle gained. This loss of the binary's orbital angular momentum decreases the separation, and is not physical. In reality, the gas would dissipate its excess kinetic energy and be captured by the binary, rather than being expelled from the system. Hence, the effects on separation due to *accretion only* must be determined. The effect due to the loss of particles is purely an artifact of modelling the cloud with ballistic particles.

The total effect of ballistic accretion on the separation of a $q = 0.6$ mass ratio binary is given in Figs. 6a and 7a with accretion radii increasing in multiples of two from $r_{\rm acc} = 0.05D$ to $r_{\rm acc} = 0.40D$. The effects on the binary's separation due to the loss of orbital angular momentum of the binary to particles that are expelled, and due to accretion, are given separately in Figs. 6b,c and 7b,c. These two separate contributions are calculated by differentiating the equation for the orbital angular momentum of the binary about its centre of mass

$$L = \sqrt{G M_{\rm b}^3 a}\,\frac{q}{(1+q)^2} \tag{10}$$

with respect to time to give

$$\dot{a} = \frac{2(1+q)^2}{q}\sqrt{\frac{a}{G M_{\rm b}^3}}\;\dot{L} - \frac{3a}{M_{\rm b}}\;\dot{M}_{\rm b} - \frac{2a(1-q)}{q(1+q)}\;\dot{q}. \tag{11}$$

The rate of change of orbital angular momentum of the binary $\dot{L}$, is contributed to both by accretion of particles and by the loss of angular momentum from the binary to the removed particles. This rate of loss of angular momentum from the binary is simple to determine from the calculations and hence its effect on the separation can be subtracted to leave the effect on separation due to accretion only. A second way to calculate $\dot{a}$ due to accretion is to keep track of the rate of increase of the orbital angular momentum of the binary due the accretion of particles, and use this in equation (11), along with $\dot{M}_{\rm b}$ and $\dot{q}$ which have already been determined. The differences in these two methods of extracting the value of $\dot{a}$ due only to accretion give the error estimates.

The removal of the effect due to particle losses from the results is critical for small-accretion-radii calculations (Figs. 6 and 7). For calculations with $r_{\rm acc} = 0.05D$, the total effect on the separation of the binary is for it to decrease in almost all cases! Only for the high $j_{\rm inf}$ does it consistently increase. Also, there are two local minima in $\dot{a}/\dot{M}_{\rm b}$. The first occurs at $j_{\rm inf} \approx 0$. The second occurs at $j_{\rm inf} \approx 1$. From Figs. 6b and 7b these minima are given predominantly by the angular momentum lost by the binary to the ballistic particles that are expelled.

For the largest-accretion-radii protostars, the loss of angular momentum to expelled particles is much lower. This is because a greater fraction of the infalling particles are accreted, and particles are accreted farther from the protostars. Thus, close encounters with the protostars, which transfer a lot of angular momentum to the particles, cannot occur. Only for $j_{\rm inf} \gtrsim 0.8$ do particle losses have a significant effect on $\dot{a}/\dot{M}_{\rm b}$. This is because the fraction of particles that are expelled (as opposed to being accreted) increases when $j_{\rm inf}$ is large.

5.2 Effects due to accretion only

Eliminating the effects from particle losses, we are left with Fig. 8, giving solely the effect of accretion of particles on the binary's separation. The most striking observation is that, generally, the graphs of $\dot{a}/\dot{M}_{\rm b}$ are monotonically increasing with $j_{\rm inf}$. Only the small-accretion-radii calculations with $q \lesssim 0.3$ break with this trend. This behaviour is expected, as the accretion of higher-angular-momentum material should

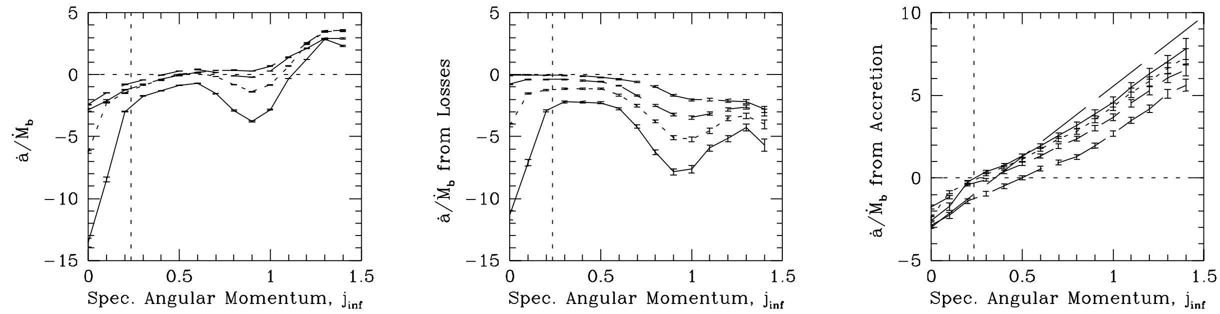

Figure 6. The rate of change of separation $\dot{a}/\dot{M}_{\rm b}$ for a $q = 0.6$ binary accreting 'gas' with specific angular momentum $j_{\rm inf}$. Shown are a) the total $\dot{a}/\dot{M}_{\rm b}$ from ballistic accretion (left), b) $\dot{a}/\dot{M}_{\rm b}$ due to loss of angular momentum to expelled particles (centre), and c) $\dot{a}/\dot{M}_{\rm b}$ due to accretion only (right). The calculations were performed with radial-infall velocity $v_{\rm rad} = 0$ and accretion radii of $r_{\rm acc} = 0.05D$ (solid), $r_{\rm acc} = 0.10D$ (dotted), $r_{\rm acc} = 0.20D$ (dashed), $r_{\rm acc} = 0.40D$ (long-dashed). The specific orbital angular momentum of the binary $j_{\rm b}$ (vertical) and the $\dot{a}/\dot{M}_{\rm b}$ expected if all the $j_{\rm inf}$ of the accreted matter was converted to orbital angular momentum and if $\dot{q} = 0$ are also given (long-dashed, right).

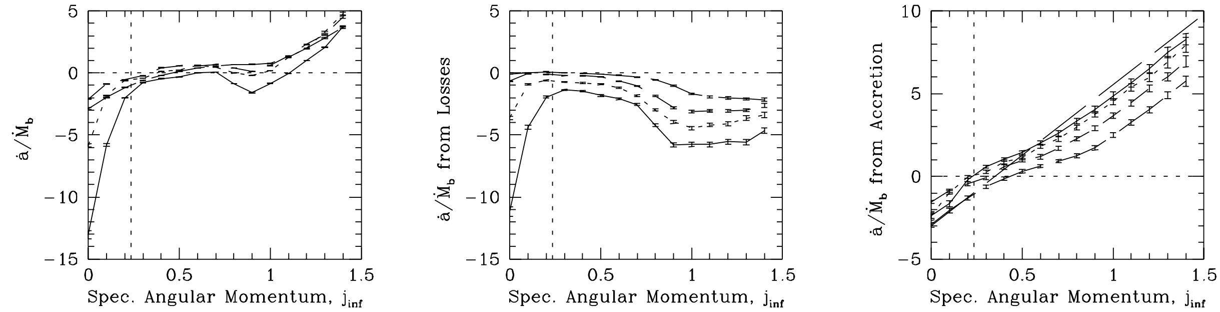

Figure 7. As in Fig. 6, except that the calculations were performed with a radial-infall velocity of $v_{\rm rad} = 1$.

increase the specific orbital angular momentum of the binary more, and thus its separation. Furthermore, for the small-accretion-radii calculations, the change from decreasing to increasing the separation occurs when the specific angular momentum of the infalling cloud material is approximately equal to the specific angular momentum of the binary

$$j_{\rm inf} \approx j_{\rm b} = \sqrt{GM_{\rm b}a}\frac{q}{(1+q)^2}, \qquad (12)$$

as is expected if the effect of $\dot{q}$ on the separation is neglected (c.f. equation (13) below). With accretion radii equal to the mean-Roche-lobe sizes, this does not happen. Instead, there is always a region where $j_{\rm inf} > j_{\rm b}$, and yet the binary's separation decreases. Also, in all cases, $\dot{a}/\dot{M}_{\rm b}$ is less for the large-accretion-radii protostars than the small. This effect is also demonstrated in Figs. 6c and 7c. As the accretion radius is increased, the rate of change of separation due to accretion decreases in nearly all cases. This dependence on the accretion radii of the protostars is because, with larger $r_{\rm acc}$, more of an accreted particle's angular momentum is converted to spin angular momentum of the protostar that accretes it, and less into orbital angular momentum (see Section 6).

To gauge how the conversion of some of the accreted material's angular momentum into spin rather than orbital angular momentum affects $\dot{a}/\dot{M}_{\rm b}$, consider equation (11). If we assume that $\dot{q} = 0$ under the accretion, and that *all* of an accreted particle's angular momentum is converted to orbital angular momentum, then

$$\frac{\dot{a}}{\dot{M}_{\rm b}} = \frac{2(1+q)^2}{q}\sqrt{\frac{a}{GM_{\rm b}^3}}\, j_{\rm inf} - \frac{3a}{M_{\rm b}}. \qquad (13)$$

This is a good approximation for $q \gtrsim 0.3$ (since then the third term in equation (11) is small even though $\dot{q} \neq 0$). This function for $\dot{a}/\dot{M}_{\rm b}$ is plotted in Figs. 6c, 7c and 8.

For high mass ratios and small accretion radii, equation (13) describes $\dot{a}/\dot{M}_{\rm b}$ well (e.g. $q = 1$, Fig. 8), demonstrating that little spin angular momentum is accreted by the binary's components. With large accretion radii, however, significant spin angular momentum is accreted, and this lowers $\dot{a}/\dot{M}_{\rm b}$.

For low mass ratios (e.g. $q = 0.1$, Fig. 8), the large $\dot{q}$ at high $j_{\rm inf}$ (e.g. $q = 0.1$, Fig. 2b) forces the small-accretion-radii calculations to deviate significantly from the prediction of equation (13) when $j_{\rm inf} \gtrsim 0.6$. The rate of change of separation is low, even though little spin angular momentum is accreted. With mean-Roche-lobe-sized accretion radii, large amounts of spin angular momentum are accreted (compared to orbital angular momentum) in addition to the effects of $\dot{q}$, and the rate of change of separation is even lower.

Changing the initial radial-infall velocity of the cloud has a negligible effect on the rate of change of separation due to accretion, for $q \gtrsim 0.3$ (Figs. 6c, 7c, and 8). For high mass ratios it is the specific angular momentum of the accreted

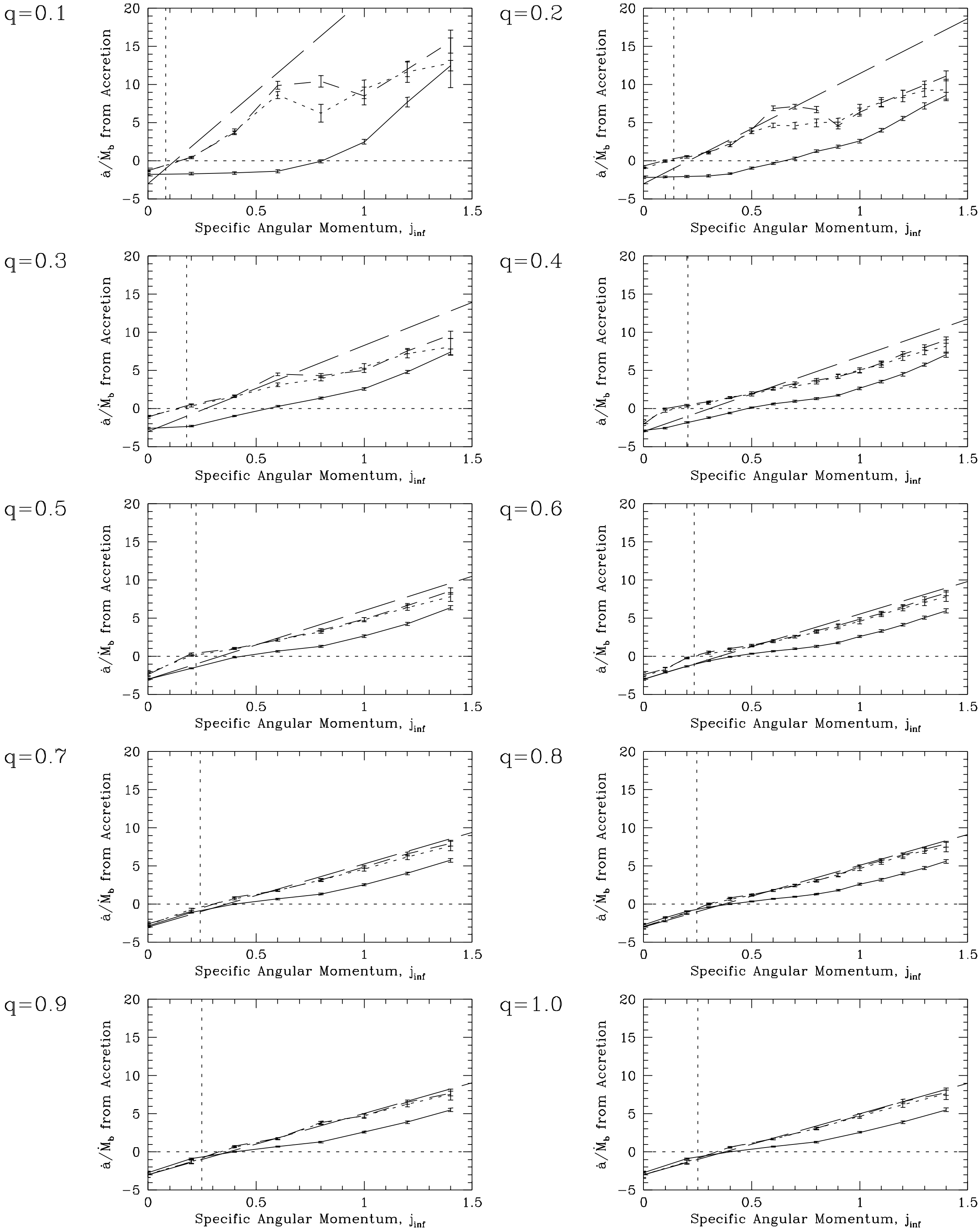

Figure 8. The rate of change of separation $\dot{a}/\dot{M}_{\rm b}$ due only to the accretion of ballistic particles for binaries with mass ratios $0.1 \leq q \leq 1.0$ accreting 'gas' with specific angular momentum $j_{\rm inf}$. The different curves are for calculations with mean-Roche-lobe-sized accretion radii $r_{\rm acc}$ and with radial-infall velocity $v_{\rm rad} = 1$ (solid), or $r_{\rm acc} = 0.05D$ with $v_{\rm rad} = 0$ (dotted) and $v_{\rm rad} = 1$ (dashed). The specific orbital angular momentum of the binary $j_{\rm b}$ (vertical) and the $\dot{a}/\dot{M}_{\rm b}$ expected if all the $j_{\rm inf}$ of the accreted matter was converted to orbital angular momentum and if $\dot{q} = 0$ are also given (long-dashed, right).

material more than the rate of change of mass ratio that affects the separation. For low mass ratios, $\dot{q}$ does affect the separation (third term in equation (11)), and hence so does the radial-infall velocity upon which $\dot{q}$ depends in the range $0.6 \lesssim j_{\rm inf} \lesssim 0.8$ for $q \lesssim 0.3$ (see Figs. 2b and 8).

Comparing the results from Figs. 6c and 7c to Artymowicz's results for the rate of change of separation of a $q=0.6$ binary (see Fig. 6 of Artymowicz (1983)), we find the closest match to his results from Fig. 7a, with $r_{\rm acc}=0.40$ and $v_{\rm rad}=1$. This again confirms the conclusion in Section 4.2, that Artymowicz used large accretion radii for his calculations. Also, judging from the form of the curves, Artymowicz probably did not attempt to take into account of the distinction between changes in the separation due to the accretion of particles, and changes due to the loss of orbital angular momentum from the binary to expelled particles which are not physical (although Artymowicz does state that this occurs). When this is taken into account, the rate of change of separation due to accretion is even more rapid than Artymowicz found for medium to high $j_{\rm inf}$.

6 ACCRETED SPIN ANGULAR MOMENTUM

In the previous section, we found the rate of change of a binary's separation depends on the relative amounts of orbital and spin angular momentum accreted by the protostars. The larger the protostellar sizes, the more of a cloud's angular momentum is converted to spin angular momentum of the protostars and the less orbital angular momentum is given to the binary. Thus, a lower rate of change of separation is obtained for binaries with larger-accretion-radii protostars.

In Figs. 9 and 10 the specific spin angular momenta of the material accreted by the protostars (s_1 and s_2 for the primary and secondary respectively) are presented as functions of $j_{\rm inf}$ for different mass ratio binaries. Indeed, the protostars with mean-Roche-lobe-sized accretion radii generally accrete far more spin angular momentum than the protostars of radius $r_{\rm acc}=0.05D$. The progression is shown clearly in Figs. 11 and 12 as the accretion radii of the protostars in a $q=0.6$ binary are increased by a multiple of two for each series of calculations. These figures also demonstrate that the accretion of spin angular momentum is insensitive to the initial radial-infall velocity at the outer boundary of the cloud.

Considering the large-accretion-radii calculations (those with mean-Roche-lobe-sized protostars, and those in Figs. 11 and 12 with $r_{\rm acc} \geq 0.20D$), the specific spin angular momentum of the accreted material varies greatly between the binary's components (for $q<1$). This occurs whether or not the protostars have equal-sized accretion radii. In most cases, for both the primary and secondary, three main regimes are apparent. First, for low $j_{\rm inf}$, in many cases, virtually no spin angular momentum is accreted by a protostar until $j_{\rm inf}$ passes a critical value (e.g. $q=0.7$, Fig. 10). This is observed for both the primary and secondary, but is generally more apparent for the secondary. Second, when $j_{\rm inf}$ is above the critical value for a protostar, the accreted specific spin angular momentum grows approximately linearly with increasing $j_{\rm inf}$. Finally, for high $j_{\rm inf}$, the linear increase with $j_{\rm inf}$ ceases and the curves level off.

The critical values of $j_{\rm inf}$, below which essentially no spin angular momentum is accreted, increase with increasing mass ratio for the primary, and decrease with increasing mass ratio for the secondary, until they converge for $q=1$ (Figs. 9 and 10). These critical values of $j_{\rm inf}$ are given by

$$j_{\rm inf} \approx j_* \quad \text{where } j_* = \begin{cases} j_1 & \text{for the primary} \\ j_2 & \text{for the secondary.} \end{cases} \tag{14}$$

They may be determined by considering the accretion process. When a particle is accreted by a protostar, it obtains the same specific orbital angular momentum as the protostar, by definition. If the accreted particle has less specific angular momentum than this before it is accreted, it must either gain specific orbital angular momentum by gravitational interactions with the protostar, and/or by giving the protostar a retrograde spin (slightly negative spin angular momentum is accreted by the protostars in some cases). If the particle has a higher specific angular momentum than the protostar, the protostar receives prograde spin angular momentum. This also explains the linear increase of the spins with increasing $j_{\rm inf}$ when $j_{\rm inf} \gtrsim j_*$. As the values of the specific angular momentum of the particles increase, more spin must be given to the protostar that accretes it in order to conserve angular momentum.

For high $j_{\rm inf}$, the linear increases of s_1 and s_2 cease due to the finite sizes of the protostellar accretion radii. This places an upper limit on the amount of spin angular momentum a particle provides when it is accreted (for a constant velocity relative to the protostar), and hence the accreted spin cannot continue to grow linearly with $j_{\rm inf}$. An equivalent statement is that particles that have a high specific angular momentum relative to a protostar are not accreted because they do not pass within the accretion radius.

Finally, in all cases where appreciable spin angular momentum is accreted, then $s_1 > s_2$ (for $q<1$). This is because $j_1 < j_2$, and the secondary's accretion radius is smaller than that of the primary. These conspire together to give a larger fraction of the angular momentum of an accreted particle to protostellar spin for the primary than for the secondary, and less to orbital angular momentum. As the mass ratio increases, these differences diminish, and lead to less protostellar spin being accreted by the primary, and more by the secondary.

7 GASEOUS ACCRETION

The effects of accretion on a protobinary have been determined by modelling the gas with ballistic particles. In reality, the accretion flow on to the binary will be affected by viscous dissipation and gas pressure. This will allow the formation of circumstellar and/or circumbinary discs which cannot occur in the ballistic calculations. Some material may be captured by the primary or secondary to form discs as opposed to actually being accreted by the protostars. The rates of change of mass of the primary and secondary must then be defined as the rates at which they capture mass. Using this definition, qualitatively, the relative accretion rate and rate of change of mass ratio are generally expected to follow the ballistic results with low-$j_{\rm inf}$ material being captured mainly by the primary, and high-$j_{\rm inf}$ material being captured mainly by the secondary. Quantitatively, the ballistic

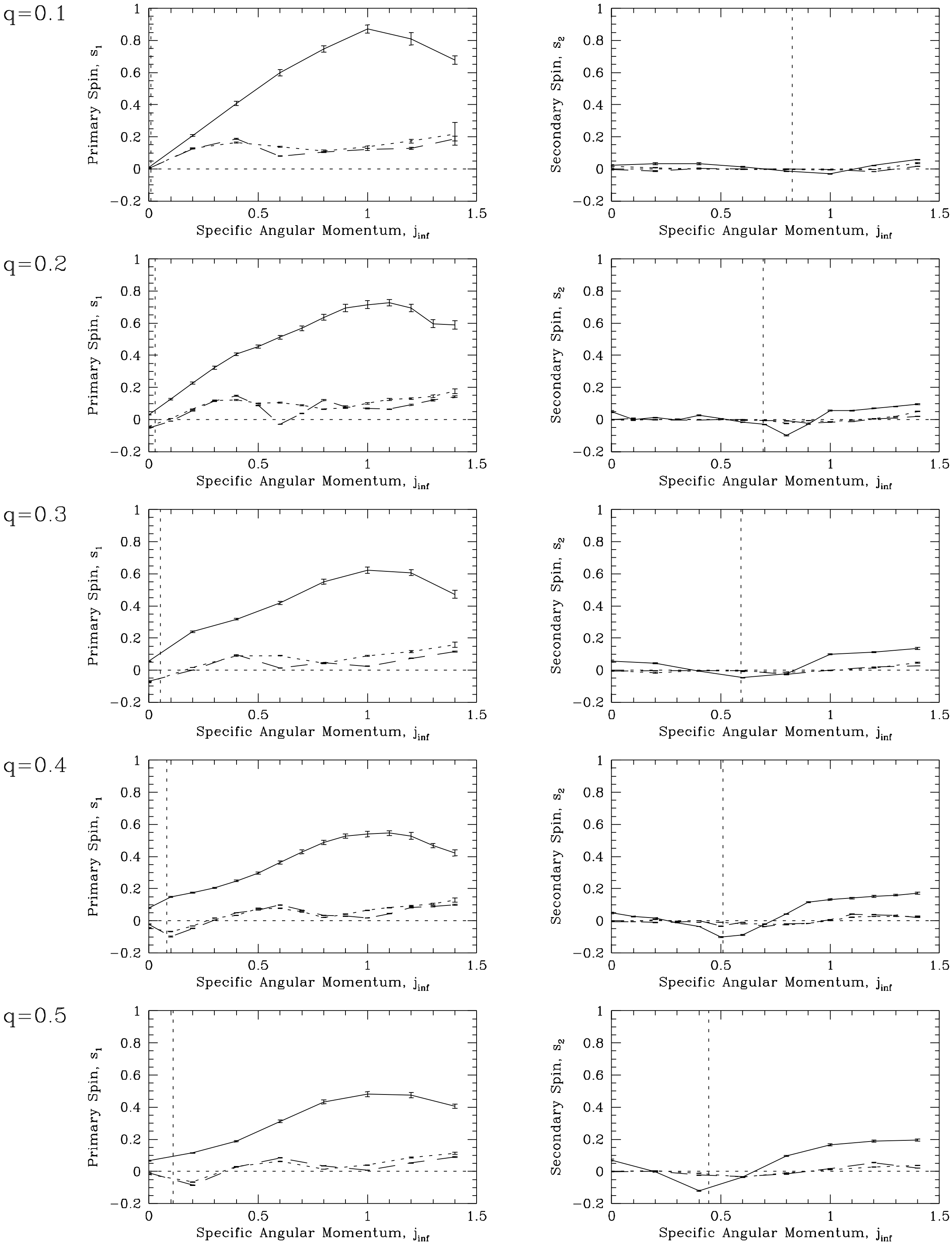

Figure 9. The specific spin angular momentum accreted by a) the primary s_1 (left) and b) the secondary s_2 (right) in binaries with mass ratios $0.1 \leq q \leq 0.5$ which accrete 'gas' with specific angular momentum $j_{\rm inf}$. The different curves are for calculations with mean-Roche-lobe-sized accretion radii $r_{\rm acc}$ and with radial-infall velocity $v_{\rm rad} = 1$ (solid), or $r_{\rm acc} = 0.05D$ with $v_{\rm rad} = 0$ (dotted) and $v_{\rm rad} = 1$ (dashed). The vertical lines give the specific orbital angular momenta of the primary j_1 (left) and secondary j_2 (right).

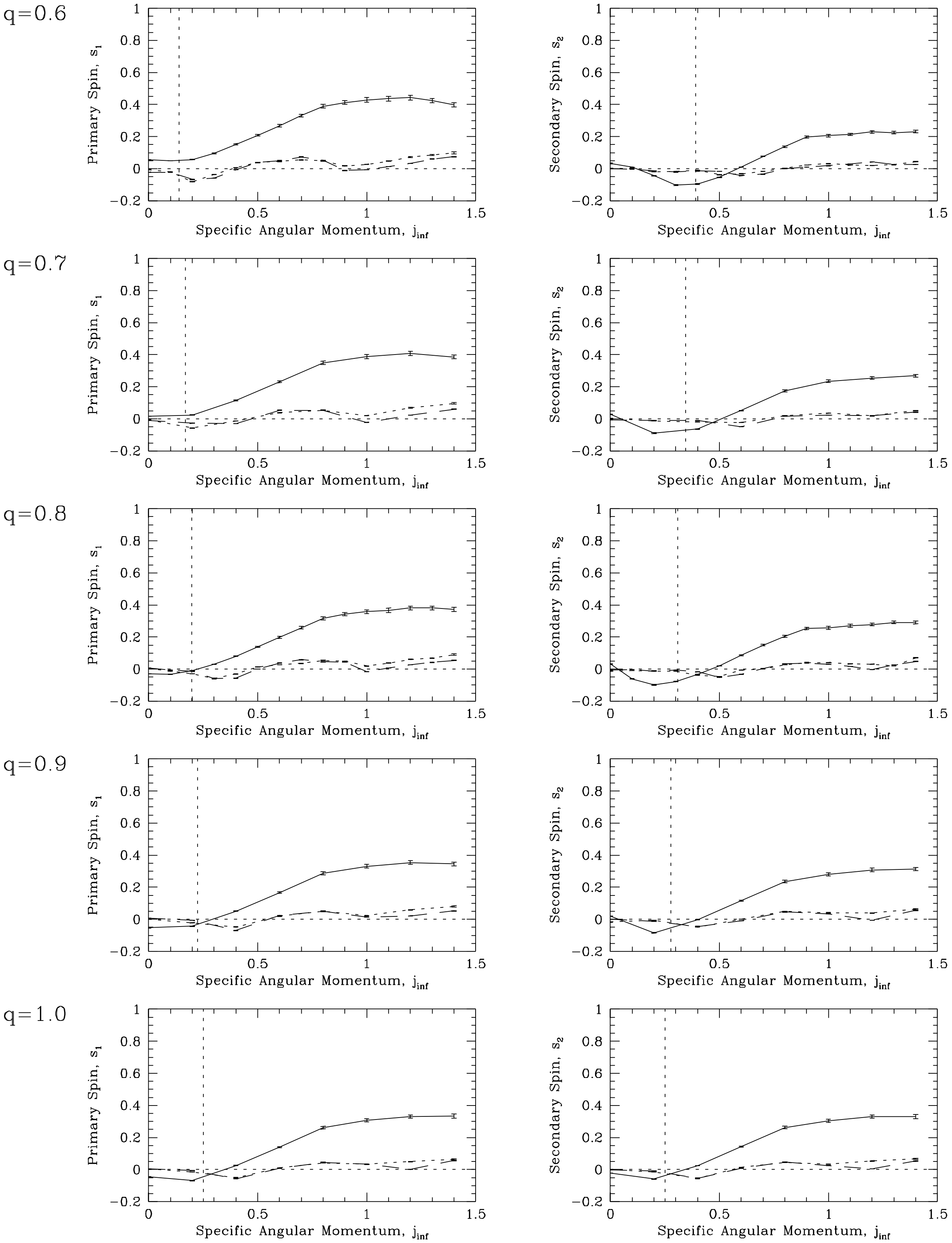

Figure 10. The specific spin angular momentum accreted by a) the primary s_1 (left) and b) the secondary s_2 (right) in binaries with mass ratios $0.6 \leq q \leq 1.0$ which accrete 'gas' with specific angular momentum $j_{\rm inf}$. The different curves are for calculations with mean-Roche-lobe-sized accretion radii $r_{\rm acc}$ and with radial-infall velocity $v_{\rm rad} = 1$ (solid), or $r_{\rm acc} = 0.05D$ with $v_{\rm rad} = 0$ (dotted) and $v_{\rm rad} = 1$ (dashed). The vertical lines give the specific orbital angular momenta of the primary j_1 (left) and secondary j_2 (right).

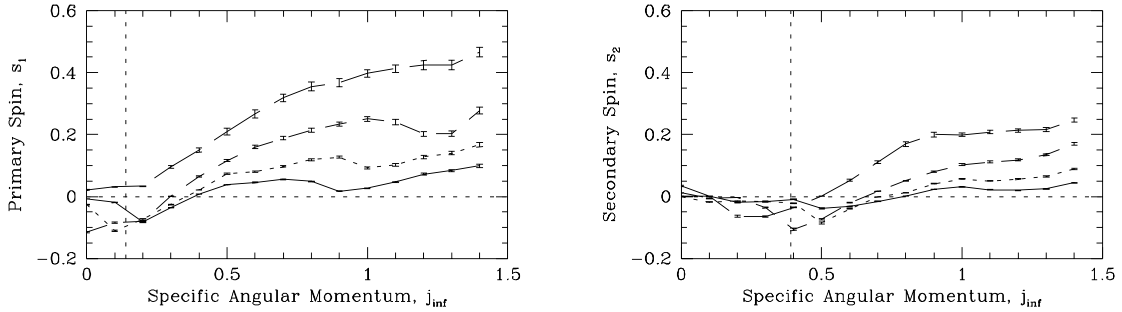

Figure 11. The specific spin angular momentum accreted by a) the primary s_1 (left) and b) the secondary s_2 (right) in a $q = 0.6$ binary which accretes 'gas' with specific angular momentum $j_{\rm inf}$. The calculations were performed with radial-infall velocity $v_{\rm rad} = 0$ and accretion radii of $r_{\rm acc} = 0.05D$ (solid), $r_{\rm acc} = 0.10D$ (dotted), $r_{\rm acc} = 0.20D$ (dashed), $r_{\rm acc} = 0.40D$ (long-dashed). The vertical lines give the specific orbital angular momenta of the primary j_1 (left) and secondary j_2 (right).

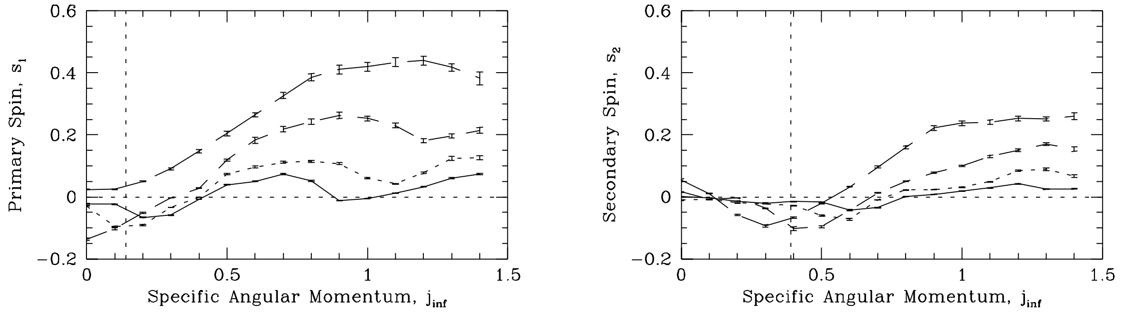

Figure 12. As in Fig. 11, except that the calculations were performed with a radial-infall velocity of $v_{\rm rad} = 1$.

results depend on the assumed accretion radii and, hence, gaseous calculations are required to determine the actual accretion rates. For $j_{\rm inf} \gtrsim 1$ the relative accretion rate is expected to be very high, since the gas will dissipate much of its radial-infall velocity in forming a circumbinary disc and we find a lower radial-infall velocity gives a higher relative accretion rate. Thus, the ballistic results may underestimate the true relative accretion rate and $\dot{q}$ in this case.

The general increase of $\dot{a}/\dot{M}_{\rm b}$ with increasing angular momentum of the cloud should be maintained with gaseous accretion. The large and small-accretion-radii ballistic results differ quantitatively, however, so gaseous calculations are again required to determine the effective sizes of the protostars. Also, the formation of a circumbinary disc for high-angular-momentum infall will affect the binary differently to ballistic accretion. For example, as mentioned above, when accreting from a circumbinary disc $\dot{q}$ is expected to be higher than for the ballistic calculations which will affect $\dot{a}$ for low mass ratios (see equation (11)). Also, the binary will lose angular momentum to the circumbinary disc via gravitational torques, decreasing the separation (Artymowicz et al. 1991).

Finally, with ballistic accretion, especially for large-accretion-radii protostars, the specific spin angular momentum that is accreted differs considerably between the two components. With gaseous accretion, material captured by the protostars that has higher specific spin angular momentum will form larger-radii circumstellar discs. Hence, circumstellar disc formation may differ considerably between the two components in a binary system, with the primary potentially having a large circumstellar disc, while the secondary has a smaller disc, or perhaps *no* disc at all. It may also be possible for retrograde discs to be formed, as, in some cases, the accreted material appears to have retrograde specific spin angular momentum relative to the cloud's specific angular momentum.

These hypotheses will be tested in a later paper where gaseous accretion on to a protobinary system is studied and compared with the ballistic results presented here.

8 CONCLUSIONS AND OBSERVATIONAL IMPLICATIONS

In conclusion, the effects of ballistic accretion on the masses and separations of initially-circular, protobinary systems have been studied for a wide range of mass ratios and values of the specific angular momentum of the infalling cloud. The qualitative behaviour of systems under ballistic accretion, determined by Artymowicz (1983), has been confirmed over this increased parameter space. First, the accretion of low-angular-momentum material decreases the mass ratio of the binary, while the accretion of high-angular-momentum material increases the mass ratio towards unity. Second, low-angular-momentum accretion decreases the separation, while high-angular-momentum accretion increases the separation. Although only circular binaries have been studied, this behaviour is expected to apply to eccentric systems as well because the qualitative effects depend on the specific angular momentum of the infall relative to the binary. For example, low-angular-momentum accretion decreases the mass ratio because the material falls to the centre of mass of the system, to which the primary is closest. This occurs for both circular and eccentric systems. In addition, Artymowicz (1983) performed calculations of accretion on to both circular and eccentric binaries and did not note any difference between their qualitative behaviour.

An implication of this behaviour for the formation of binary stars is that binaries with medium to wide separations may be expected to exhibit a wide variety of mass ratios, whereas close binaries may commonly have mass ratios near unity. This distinction occurs because the material falling on to a close binary system during its formation may be expected to have high values of specific angular momentum relative to the binary, hence driving the mass ratio towards unity. This is especially true if close binaries are formed via disc fragmentation. For wide systems, on the other hand, the infalling material is more likely to have low values of specific angular momentum relative to the binary. This is in good agreement with the observational results of Duquennoy & Mayor (1991) and Mazeh et al. (1992), although better statistics on the mass ratios of close binaries are required.

Artymowicz (1983) found the quantitative results to be relatively insensitive to the initial radial-infall velocity of the material at the outer boundary of the calculation. The results presented here agree with this conclusion, with the exception of high-angular-momentum infall. In this case, the radial-infall velocity of the infalling gas is critical in determining the relative accretion rate and thus the rate of change of mass ratio of the binary. In most cases, the radial-infall velocity does not significantly affect the rate of change of separation of the binary. The exception to this is for low mass ratio binaries ($q \lesssim 0.3$) where the rate of change of separation also depends on $\dot{q}$ and this depends on the radial-infall velocity.

Contrary to Artymowicz, the quantitative results are found to depend *critically* on the assumed sizes of the protostars. For large-radii protostars, the relative accretion rates and rate of change of mass ratio are less extreme than for small protostars. Also, for large protostars, more of the accreted angular momentum is converted to spin angular momentum of the protostars rather than orbital angular momentum, so that the rate of change of separation is lower for binaries containing larger protostars. Thus, for quantitative results to be obtained the appropriate effective sizes of the protostars must be determined. This is presumably some combination of the physical sizes of the protostars (for close binaries), and circumstellar disc sizes (for more widely separated binaries). The only way to obtain these sizes is to include hydrodynamical effects in the calculations.

Finally, analysis of the specific spin angular momentum accreted by each component of a protobinary suggests that disc formation around the two components may differ considerably. For large-accretion-radii protostars, the material captured by the primary nearly always has enough specific spin angular momentum to form a significant circumstellar disc. For the secondary, the captured material always has less specific spin angular momentum than that captured by the primary, and in many cases may not form a circumsecondary disc at all.

ACKNOWLEDGMENTS

I am indebted to Cathie Clarke for her suggestion that this problem be studied, and I am grateful to her, Ian Bonnell and Jim Pringle for many enlightening discussions. I also thank Cathie Clarke, Ian Bonnell and Melvyn Davies for their critical reading of various versions of the manuscript. Finally, I am grateful to the IoA system managers for their dedication to providing the best possible computing resources. I also acknowledge scholarships from the Cambridge Commonwealth Trust and the William Georgetti Memorial Trust, an ORS award, and financial support from the Max-Planck-Institut für Astronomie, Heidelberg where this paper was written.

REFERENCES

Adams F. C., Ruden S. P., Shu, F. H., 1989, ApJ, 347, 959
Artymowicz P., 1983, Acta Astronomica, 33, 223
Artymowicz P., Clarke C. J., Lubow S. H., Pringle J. E., 1991, ApJ, 370, L35
Bate M. R., 1995, Ph.D. thesis. University of Cambridge, Cambridge
Bate M. R., Bonnell I. A., Price N. M., 1995, MNRAS, 277, 362
Bonnell I. A., 1994, MNRAS, 269, 837
Bonnell I., Bastien P., 1992, ApJ, 401, 654
Bonnell I. A., Bate M. R., 1994a, MNRAS, 269, L45
Bonnell I. A., Bate M. R., 1994b, MNRAS, 271, 999
Bonnell I., Arcoragi J. -P., Martel H., Bastien P., 1992, ApJ, 400, 579
Bonnell I., Martel H., Bastien P., Arcoragi J. -P., Benz W., 1991, ApJ, 377, 553
Boss A. P., 1986, ApJS, 62, 519
Boss A. P., Bodenheimer P., 1979, ApJ, 234, 289
Burkert A., Bodenheimer P., 1996, MNRAS, in press
Duquennoy A., Mayor M., 1991, A&A, 248, 485
Fischer D. A., Marcy G. W., 1992, ApJ, 396, 178
Frank J., King A. R., Raine D. J., 1985, Accretion Power in Astrophysics. Cambridge University Press, Cambridge, p. 56
Ghez A. M., Neugebauer G., Matthews K., 1993, AJ, 106, 2005
Heemskerk H. M., Papaloizou J. C., Savonije G. J., 1992, A&A, 260, 161
Kopal, Z., 1959, Close Binary Systems (International Astrophysics Series, Vol. 5). Chapman & Hall Ltd., London, p. 79-80
Leinert Ch., Weitzel N., Zinnecker H., Christou J., Ridgeway S., Jameson R., Haas M., Lenzen R., 1993, A&A, 278, 129
Mathieu R. D., Walter F. M., Myers P. C., 1989, AJ, 98, 987
Mayor M., Duquennoy A., Halbwachs J. -L., Mermilliod J. -C., 1992, in McAlister H. A., Hartkopf W. I., ed., Complementary Approaches to Double and Multiple Star Research (IAU Colloquium 135). ASP, San Francisco, p. 73
Mazeh T., Goldberg D., Duquennoy A., Mayor M., 1992, ApJ, 401, 265
Myhill E. A., Boss A. P., 1993, ApJS, 89, 345
Nelson R., Papaloizou J. C., 1993, MNRAS, 265, 905
Reipurth B., Zinnecker H., 1993, A&A, 278, 81
Shu F. C., Tremaine S., Adams F. H., Ruden S. P., 1990, ApJ, 358, 495
Simon M., Chen W. P., Howell R. R., Slovik D., 1992, ApJ, 384, 212
Woodward J. W., Tohline J. E., Hachisu, I., 1994, ApJ, 420, 247